

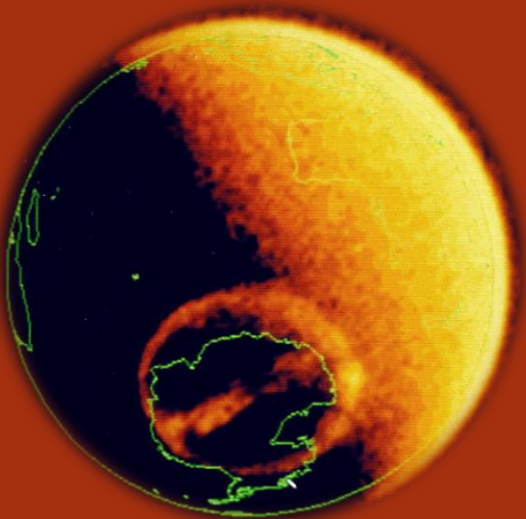
STATISTICS OF TRANSPOLAR ARCS IDENTIFIED BY AN AUTOMATED DETECTION ALGORITHM.

G.E.Bower¹ (geb21@leicester.ac.uk) S.E.Milan^{1,2}, L.J.Paxton³ and S.M. Imber¹

¹ University of Leicester, UK

² Birkeland centre for space science, Bergen, Norway

³ Johns Hopkins University applied physics laboratory, USA

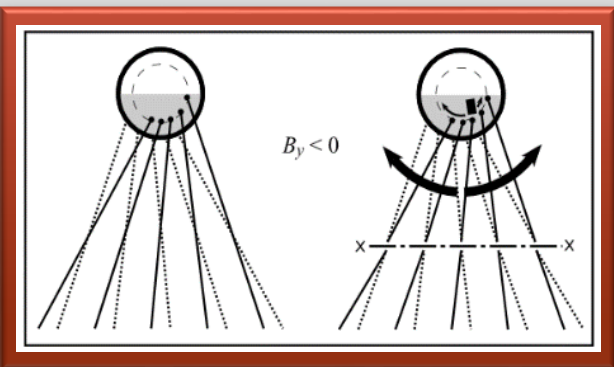


FORMATION MODELS: CLOSED OR OPEN FIELD LINES?

Transpolar arcs or TPAs are an auroral phenomena which lie poleward of the main auroral oval where aurora do not usually form. And occur during Northward IMF, such that reconnection take place in the lobes of the magnetosphere. There is currently no unanimously agreed upon formation model. There are two main theories for TPA formation. One based on closed field lines another based on open field lines.

Closed

- The Milan et al 2005 model suggests that TPAs are produced by tail reconnection as shown in figure 1.
- In a tail twisted by IMF B_y -associated stresses, some of the flux becomes trapped and protrudes into the polar cap.



- In this case TPAs form conjugately in both hemispheres but reflected across the midnight meridian.

Open

- Precipitation producing the visual arcs is embedded in a high-density polar rain originating in the solar wind.
- The TPA is expected to form due to polar cap flow shears which produce field aligned currents (FACs).
- In this case there is no reason for TPAs to form conjugately in both hemispheres (Zhu et al 1997).

Figure 1) schematic of tail field lines, before and after tail reconnection, for the cases of $B_y < 0$ (Milan et al., 2005).

DMSP/SSUSI DATA

- Spacecraft F16, F17 and F18.
- 100 min orbit.
- ~20 min to build up a image of a swath of the auroral region by scanning anti-sunward along its orbit.
- Operates at five wavelengths shown in table 1.
- Three spacecraft together provide nearly simultaneous observations of both hemispheres.
- An example of A TPA detected in the DMSP/SSUSI data is shown in figure 2.

Name	Lyman- α	Oxygen line	Oxygen line	LBHs	LBHI
Wavelength (nm)	121.6	130.4	135.6	140-150	165-180

Table 1) wavelengths observed by DMSP/SSUSI

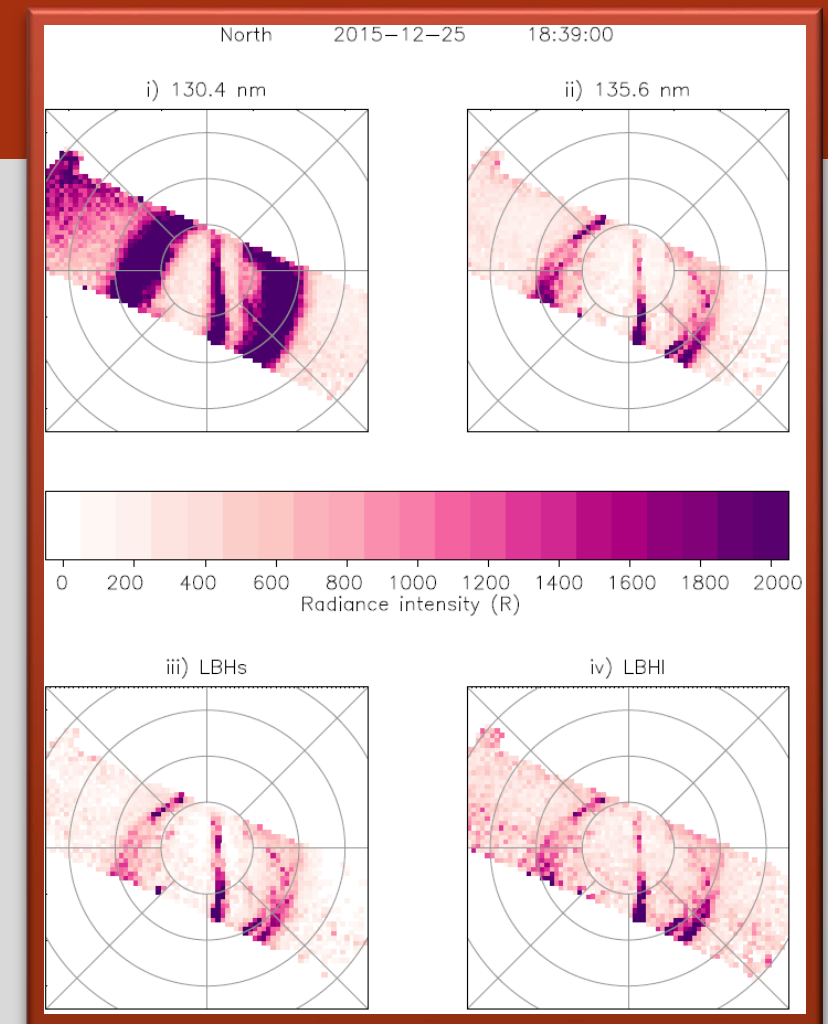


Figure 2) F16 SSUSI data on the 25th December 2015 in the Northern Hemisphere

DETECTION ALGORITHM

The detection algorithm only uses 4 out of the 5 wavelengths used by SSUSI. The two oxygen wavelengths and the LBH bands. As the Lyman alpha data is poor in comparison to the others.

Steps

1. Identify the detection window, the area above 12.5° colatitude (black circle).
2. Average the radiance intensity (vertically in figure 3 faint grey line).
3. Smooth the data using boxcar method (black line in figure 3).
4. Test maximum and minimum values against the upper and lower quartile respectively of the average radiance intensity of whole of 2015.
5. If the maximum and minimum found lie outside these values for two or more of the wavelengths a potential arc is identified.
6. Arcs are then checked by eye to remove any false positives including bending arcs which appear visually similar but form differently.
7. The location of the maximum radiance intensity across the dusk-dawn meridian is also recorded.

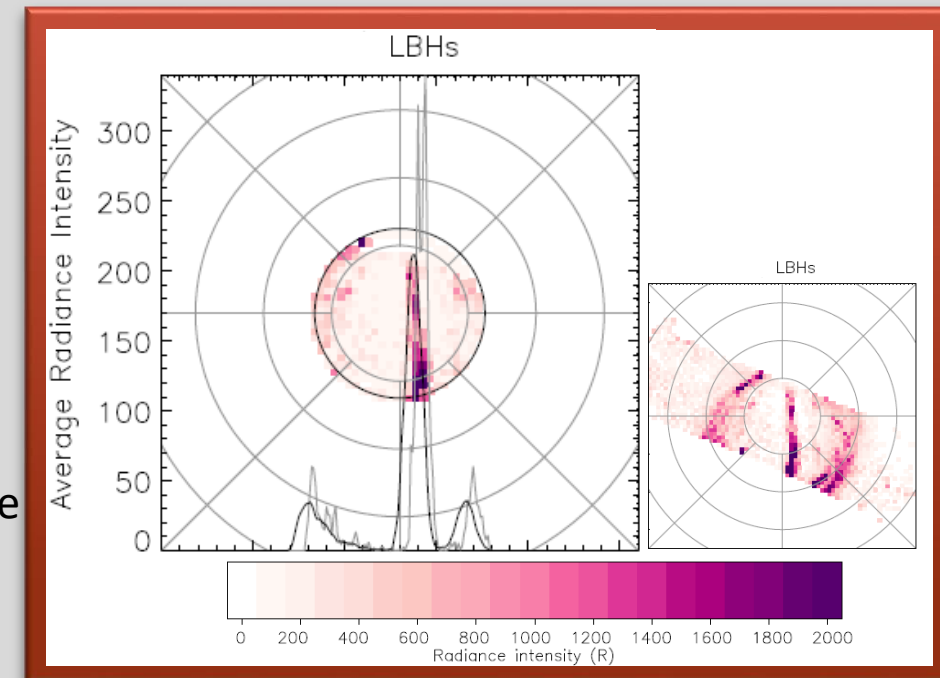


Figure 3) Detection algorithm

FALSE POSITIVES

Figures 4 show different examples of false positives with images in the four wavelengths.

- Figure 4a is when SSUSI has a high intensity over the majority of the image, probably due to sunlight contamination
- Figure 4b is when the main auroral oval enters the detection window and is misinterpreted as a TPA. This occurs most often when the dawn oval is at very high latitudes.
- Figure 4c is when the whole detection window is not scanned and a part is left untested, therefore an insufficient area of the polar cap is sampled to give a reliable measure of the average radiance intensity.
- Figure 4d is a bending arc.

Also, F17 has a very poor response at 130.4 and 135.6 nm line emission due to an issue in the grating which leads to some false positives.

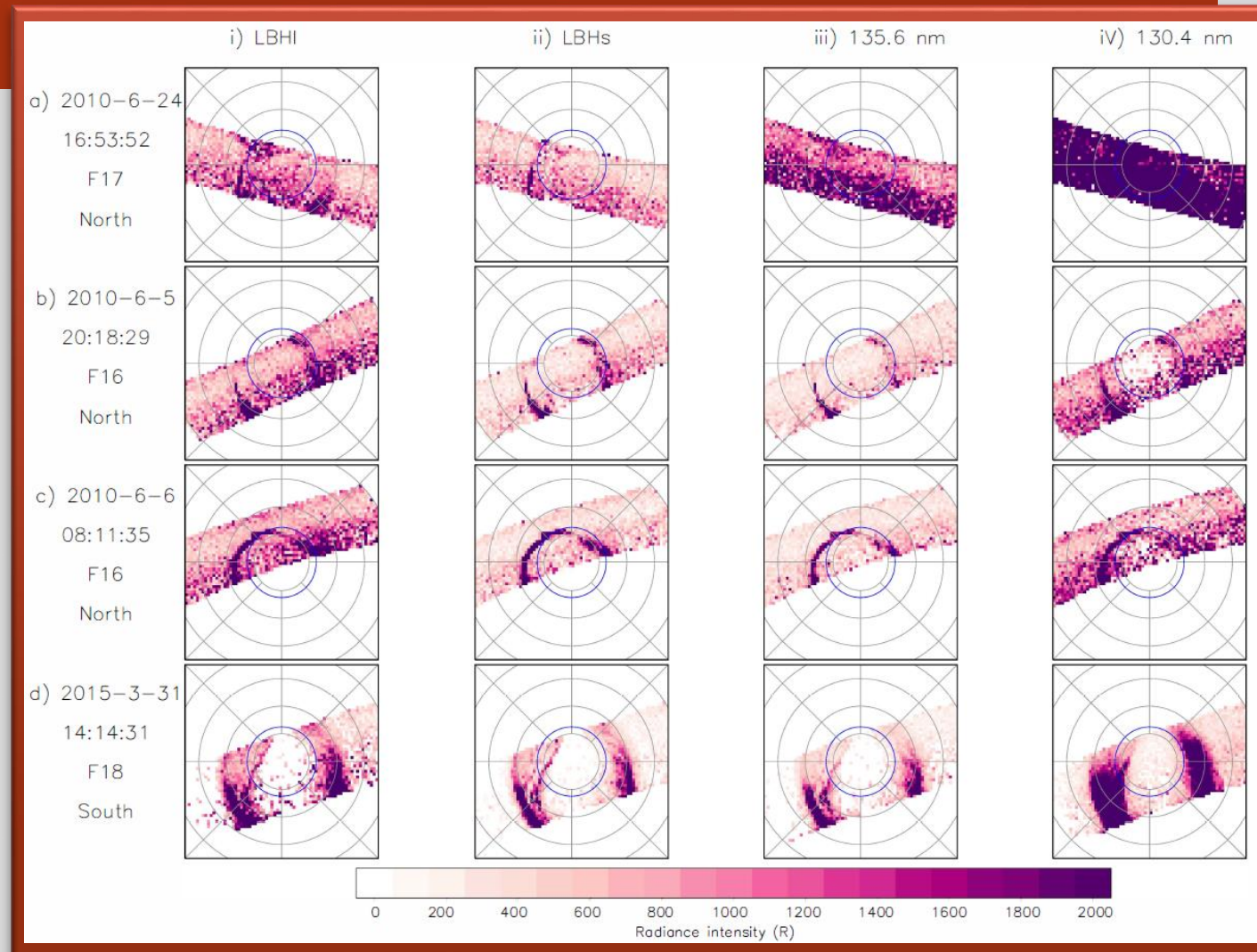


Figure 4) False positive detections. (a) High intensity over the whole image. (b) Auroral oval enters detection window. (c) Detection window is not fully imaged. (d) Bending arc. The blue circle represents the detection window of the detection algorithm.

TPA IMAGES

First we consider each TPA image individually.

NUMBER OF TPA IMAGES BY MONTH

- The detection algorithm was used between 2010 and 2016 identifying over 5500 TPAs SSUSI images
- Figure 5 shows a break down of these by month and year. It can be seen that the occurrence peaks in February and October-November.

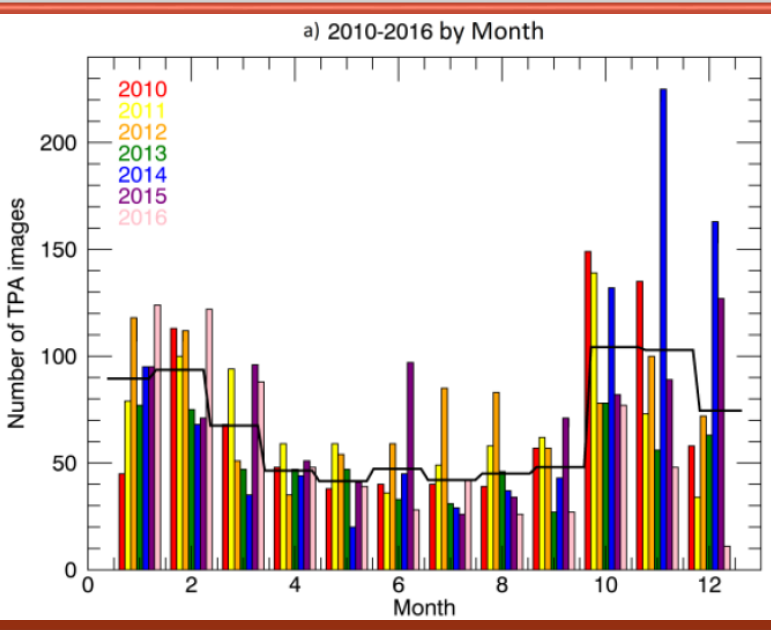


Figure 5) TPA images by month and year. Black line is the average for each month.

- When we consider the average value of the northward IMF B_z between 2010 and 2016 (Figure 6a) we find the peaks to be in February and November the same as our occurrence of TPAs.
- Tang et al. (2020) found that their TPAs were more likely to occur when the northward component of the IMF is greater than 2 nT.
- From Figure 6b we can see that northward IMF peaks in February and October-November are the same as when the number of TPA images peaks.

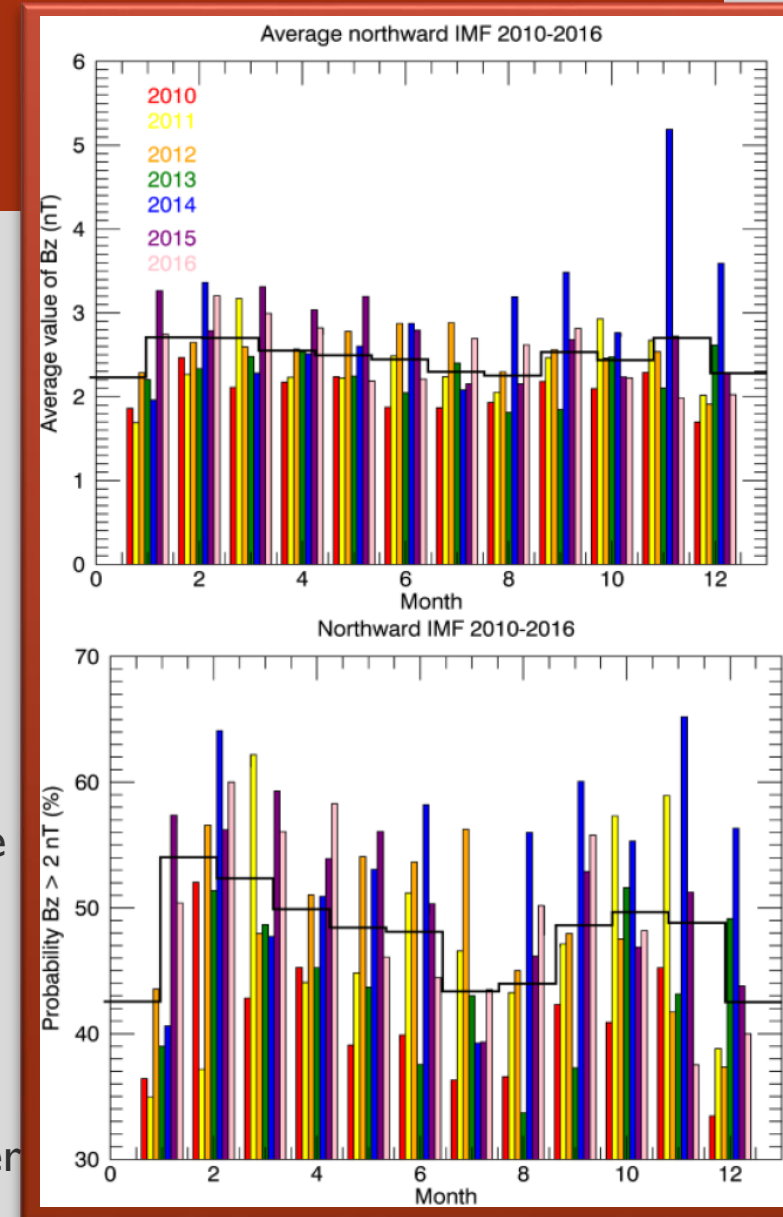


Figure 6) Detection algorithm

NUMBER OF TPA IMAGES BY HEMI

We have split the TPA images by hemisphere (northern hemisphere is red and southern hemisphere in blue) and by month in figure 7a and by UT in figure 7b. Both of these figures show distinct distributions.

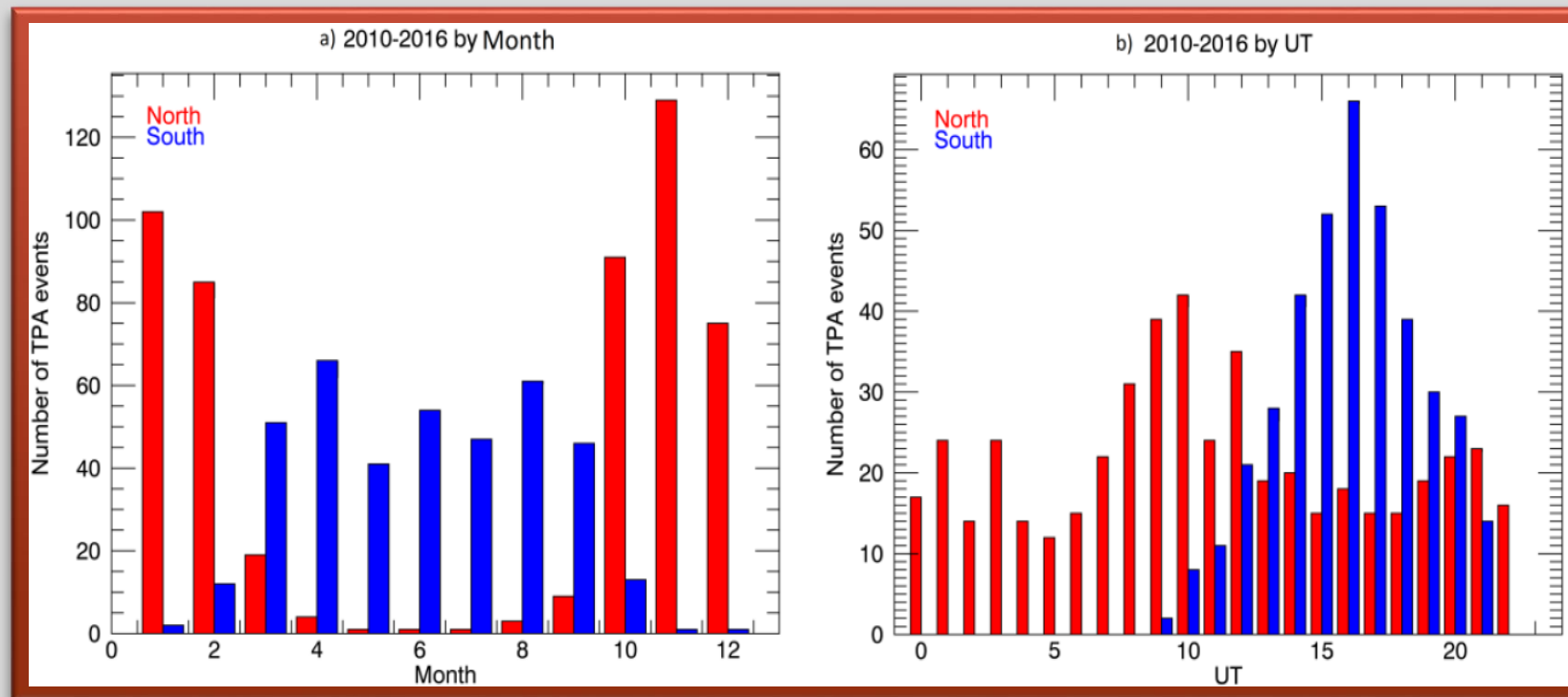


Figure 7) TPA images by hemisphere. Northern hemisphere indicated in red and southern hemisphere in blue. a) By month. b) By UT.

More TPA images
identified in the
winter hemisphere

Southern hemisphere
arcs only seen between
~ 9 and 23 UT

In an attempt to understand these distributions, the area scanned by SSUSI was considered. Here the focus is on F16 but F17 and F18 follow a similar pattern.

UT ORBITAL BIASES: F16

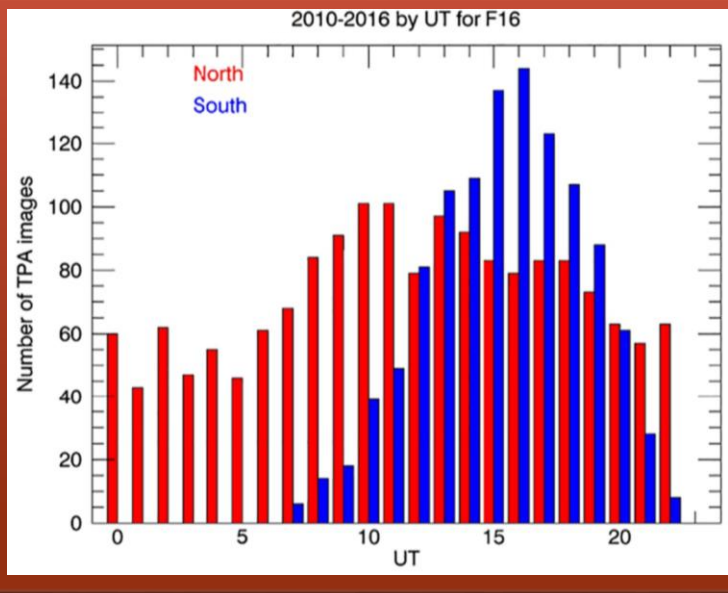


Figure 8) Number of TPA images identified by F16 by hemisphere and UT.

Figure 8 is the UT distribution for the TPAs identified by F16. This shows a very similar distribution to figure 7b which was for TPAs identified by all three spacecraft.

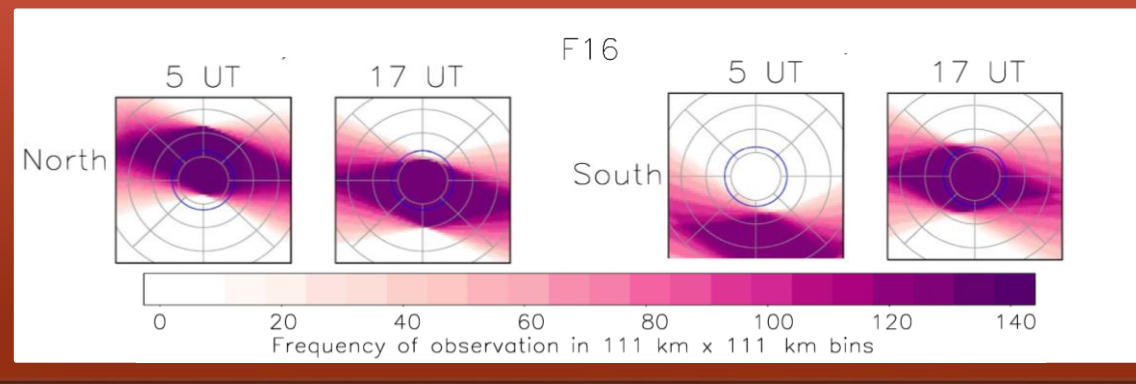


Figure 9) The frequency of the area scanned by F16-SSUSI for 5 and 7 UT for January in the northern and southern hemisphere.

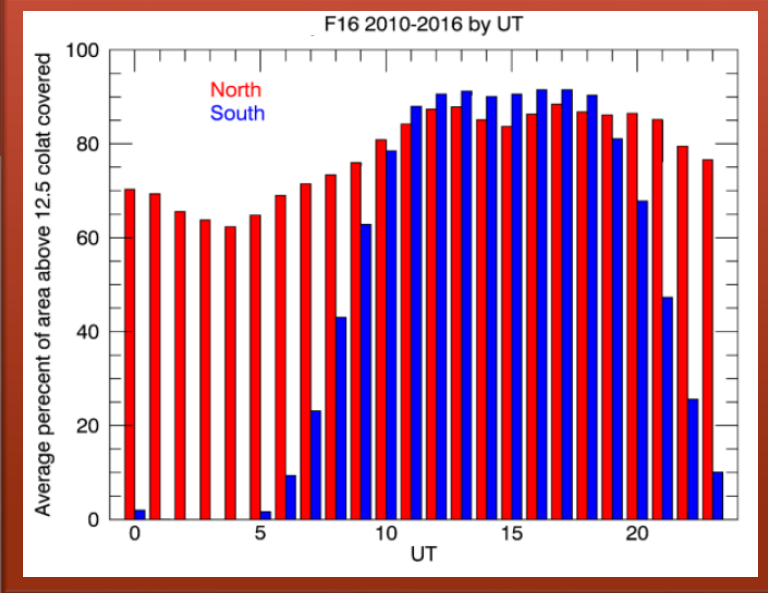


Figure 10) Average percent of tested area scanned by F16 at each UT.

The gradual change of spacecraft track with respect to the earth can explain the dependence in UT for both the northern and the southern hemisphere. Figure 10 uses all the F16 SSUSI images not just the TPA images and shows the average percent of the area above 12.5° that is scanned by SSUSI.

The similarity between figure 8 and figure 10 confirms that the UT dependence is linked to the orbital bias of the scan of the detection window.

MONTHLY ORBITAL BIASES: F16

(The figure are in the same format as the previous slide.)

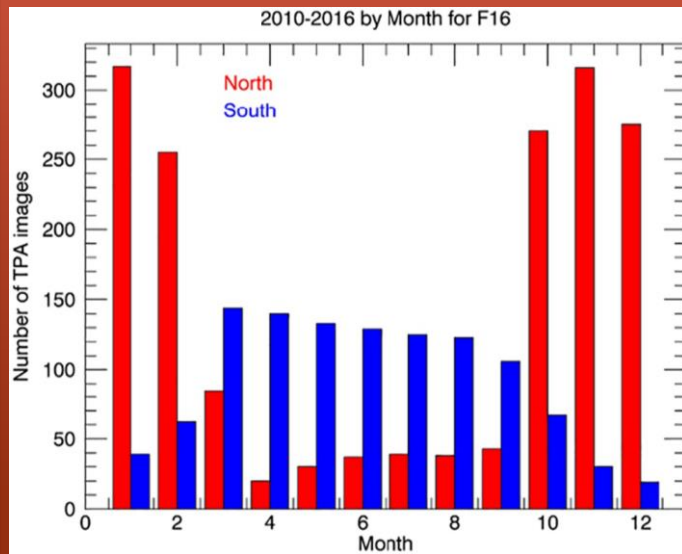


Figure 11) Number of TPA images identified by F16 by hemisphere and Month.

Figure 11 shows the frequency that the area is scanned by F16-SSUSI for northern and southern hemisphere for June and December of each year between 2010 and 2016.

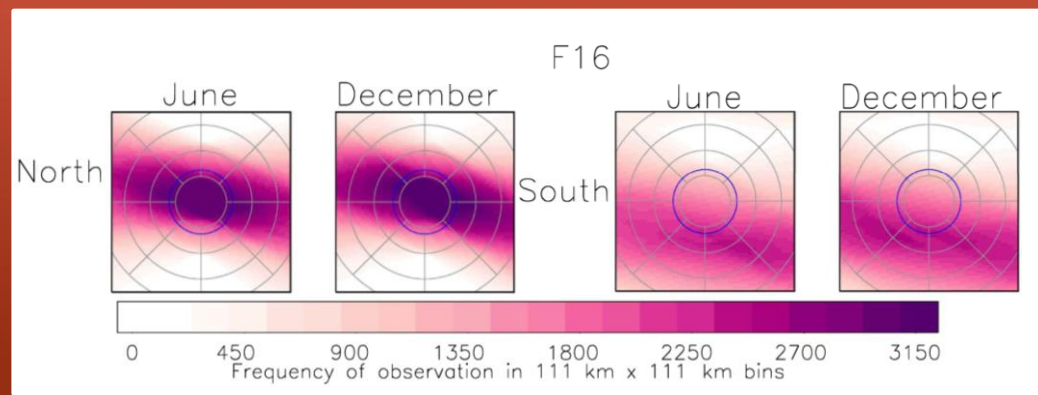


Figure 12) The frequency of the area scanned by F16-SSUSI for June and December in the northern and southern hemisphere

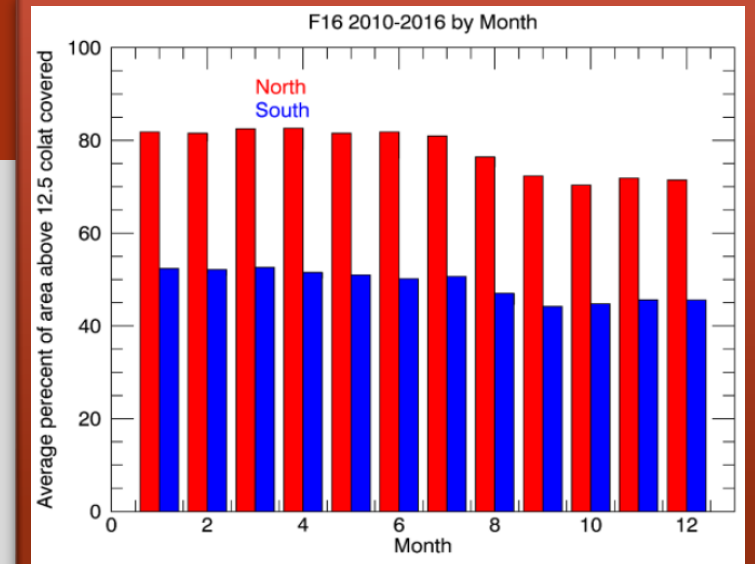


Figure 13) Average percent of tested area scanned by F16 at each month

Figure 13 shows the average percent of the tested area above 12.5 degree colatitude scanned for all of the F16 SSUSI images. As seen from figure 12 the tested area used by the detection algorithm isn't scanned as frequently in the southern hemisphere as in the northern hemisphere. As such more TPAs are detected in the northern hemisphere.

It is clear that the orbital bias of the scan of the detection window do not lead to the seasonal dependence, as figure 11 and 13 are distinctly different.



TPA EVENTS

TPA events are groups of TPA images which we believe constitute observations of the same TPA by one or more spacecraft in the northern and/or southern hemisphere.

NUMBER OF TPA EVENTS

- Figure 14a and 14b show the number of one-hemisphere TPA events by month and by UT, respectively.
- This has not been taken into account if the viewing is poor in the other hemisphere.
- The same variation is seen here as in Figure 7 such that there are more TPA events identified in the winter hemisphere and there are fewer TPA events in the southern hemisphere between 23–09 UT and a peak around 17 UT.
- Figures 14c and 14d show the number of two-hemisphere TPA events by month and by UT, respectively.
- More TPAs are identified in February and October, and the UT distribution follows a similar pattern to the southern hemisphere of the one-hemisphere events.

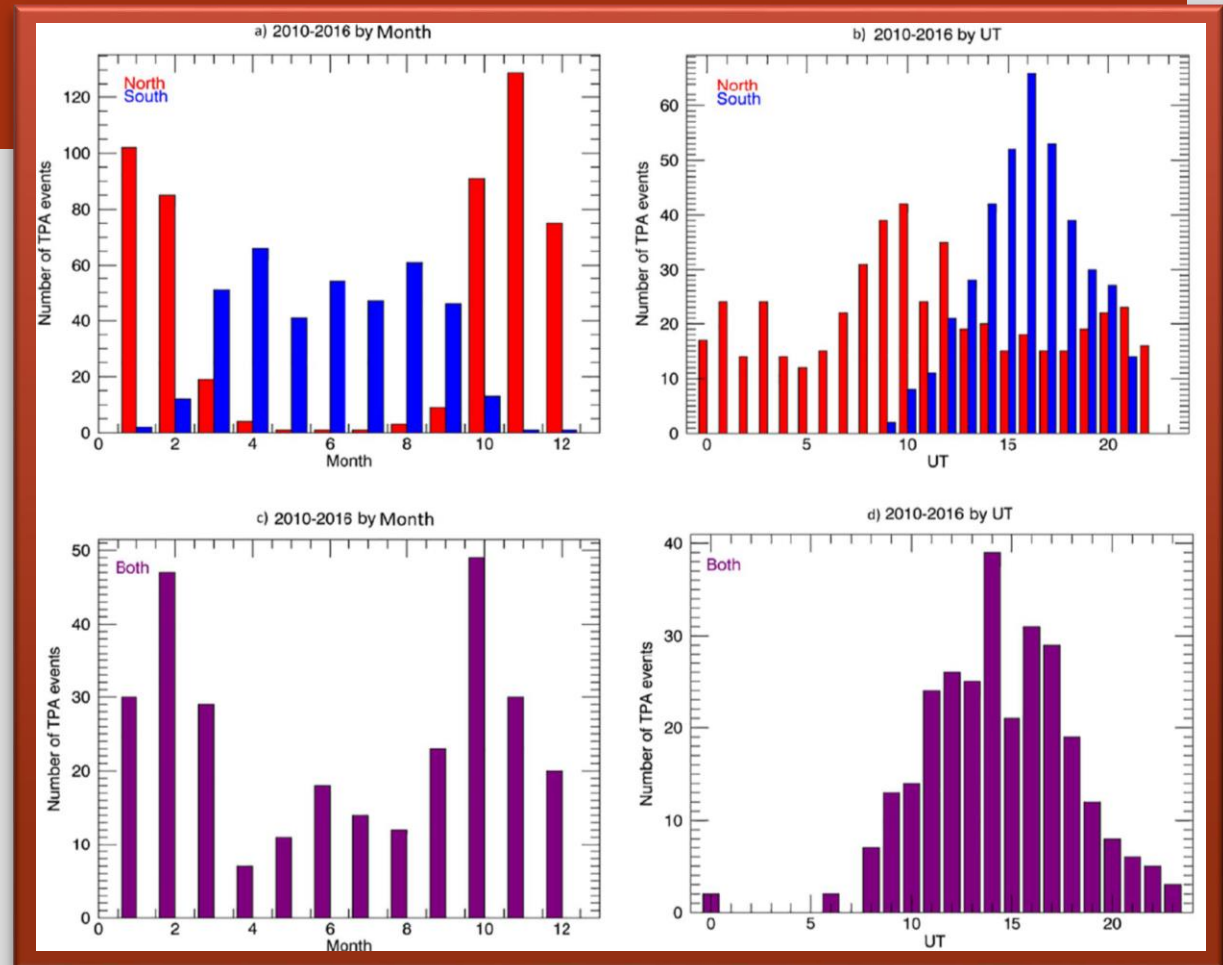


Figure 14) Number of transpolar arc (TPA) events per hemisphere combining all TPA events from 2010-2016 by (left panels) number of TPA events by month and (right panels) number of TPA events by UT. (a-b) One hemisphere events, the northern hemisphere is red and southern hemisphere blue. (c-d) Both hemisphere events, in purple.

LOCATION OF TPA

The location of the peak in average radiance intensity is recorded by the detection algorithm and is used as a proxy of the location of the TPA across the dusk-dawn meridian,

DUSK-DAWN COMPARISON

- Figure 15a is the dusk-dawn distribution of the TPA images. The error bars come from the fact that the peak intensity isn't always in the central location of the arc and can be skewed slightly.
- We compared our dusk-dawn distribution, shown in grey in figure 15b, with that of other studies that provide enough information to determine their dusk-dawn distributions.
 - Hosokawa et al. (2011) used all-sky imager at resolute bay Canada between January 2005 and December 2009.
 - Fear et al. (2012) used IMAGE data between June 2000 and September 2005.
 - Rairden and Mende (1989) used all-sky camera located at the south pole station April and August 1983-1986.
- It can be seen that there is always a preference for TPAs to be identified in dawn sector.

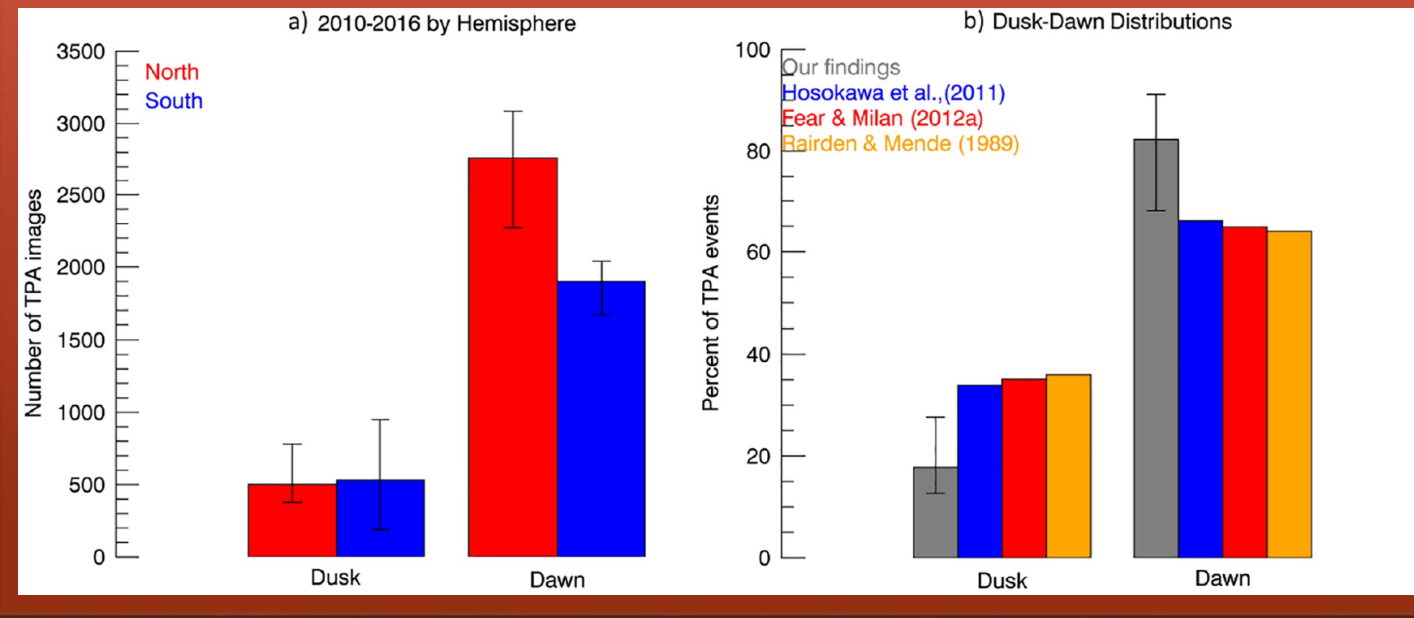


Figure 15) a) Number of TPA images by location and hemisphere. b) Number of TPA images at dusk and dawn for several studies. Ours (grey), Fear and Milan 2012a (red), Hosokawa et al 2011 (blue), Rairden and Mende 1989 (yellow).

- This could be linked to the FAC polarity. As during northward IMF there is a region of convergent electric fields on the dawn side for both positive and negative values of B_y . Therefore leading to a region of upward current on the dawnside of the polar cap and a region of downward current on the duskside. This allows the flow of more intense electron fluxes in the dawnside thus brighter auroral emission is expected therefore more TPAs would be expected to be detected in the dawn sector as seen.

PROBABILITY

- Assuming that TPAs occur uniformly throughout the year the northern and southern hemisphere distributions can be treated as the probabilities of seeing an arc if it is present in the given hemisphere
- The probabilities are defined such that the probability is one in the month with the greatest number of TPAs detected.
- The expected probability of seeing a TPA in both the northern and southern hemisphere simultaneously is then the probability of seeing a TPA in the northern hemisphere multiplied by the probability of seeing the TPA in the southern hemisphere (the red and blue lines, multiplied). This is shown by the black dashed line in Figures 16a, suitably scaled. Figures 16b is the same analysis but for the UT distributions.

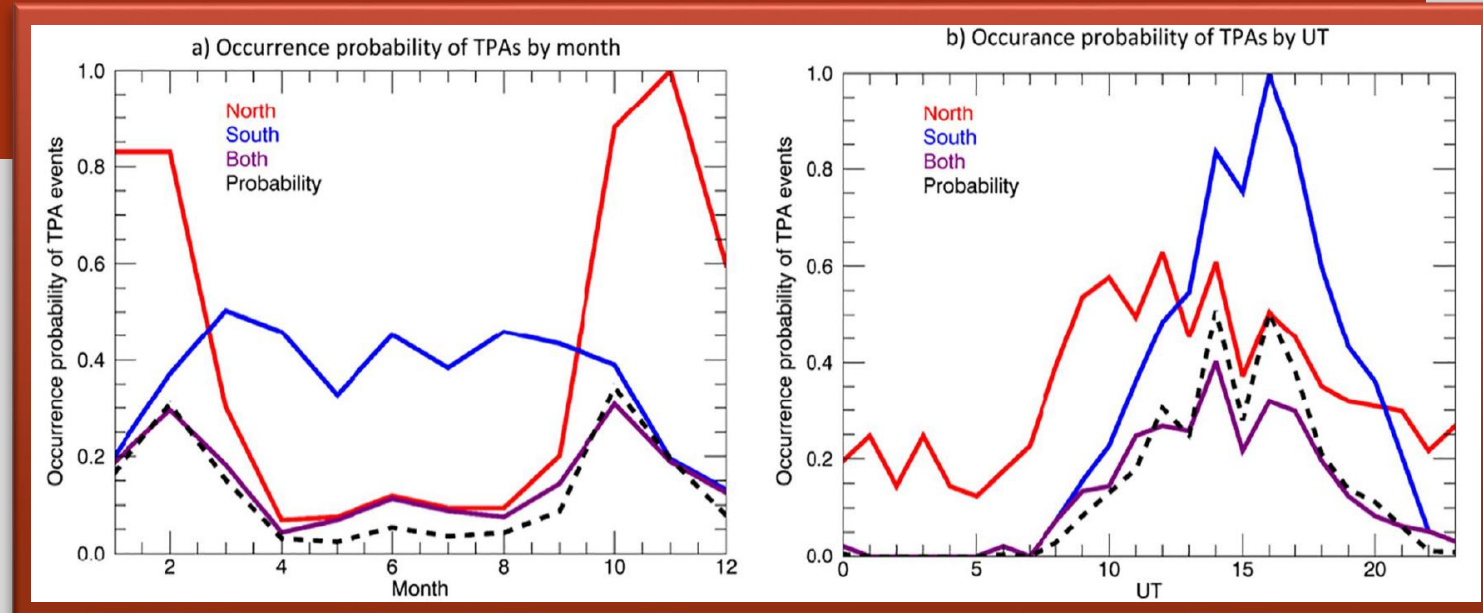


Figure 16) Probability distributions. (a) By month. (b) By UT. The red (blue) line is the northern (southern) hemisphere transpolar arc (TPA) events include those seen in a singular hemisphere and those seen simultaneously in both hemispheres. The purple line is the TPA seen simultaneously in both hemispheres. The black dashed line is the probability of a TPA being detected in both hemispheres..

- There is good agreement between the observed simultaneous events (purple lines) and the distributions modelled on probabilities (black lines).
- This suggests that the distribution of the both hemisphere events can be treated as a visibility issue.
- Therefore there is no need to invoke different formation mechanisms for one-hemisphere and two-hemisphere events.

IN RELATION TO FORMATION MODELS

If the fields are closed and the Milan et al. (2005) model is correct

- ▶ We would expect to see the TPA in both hemispheres simultaneously. Possibilities for the seasonal dependence are then as follows
 - ▶ Seasonal change in visibility of TPA. It would be expected that the TPAs could not be seen against the brightness of the sunlit hemisphere.
 - ▶ Auroral signature of TPAs is seasonally dependant, that they do not as manifest in summer this could be related to the conductance of the ionosphere.
 - ▶ Mapping of closed flux is different in the two. However, why the winter hemisphere would be preferred is not understood.

If the field lines are instead open

- ▶ No need for the TPA to be in both hemispheres simultaneously
- ▶ The seasonal dependence could be explained if polar cap flow shears that produce FACs and hence TPAs are preferentially found in the winter hemisphere. Although It is unclear why the flow shears would be preferentially found in the winter hemisphere.

Neither model suggests a preference for Dawn TPAs therefore, we suggest that this requires a revision of our understanding of TPA formation to account for this.

CONCLUSIONS

- Our TPA statistics are in agreement with other studies.
- The UT distribution seen in the results can be explained by the area used by the detection algorithm not always being scanned by SSUSI.
- No seasonal orbital bias has been found for these spacecraft.
- We suggest that field-aligned current polarity may play a role in the observed asymmetry, and suggest that this requires a revision of our understanding of TPA formation.

This work has been published in JGR: space physics therefore further detail of the work can be found at DOI: 10.1029/2021JA029743

References :

Fear, R. and Milan, S. (2012a). The IMF dependence of the local time of transpolar arcs: Implications for formation mechanism. *Journal of Geophysical Research: Space Physics*, 117(A3). <https://doi.org/10.1029/2011JA017209>

Hosokawa, K., Moen, J., Shiokawa, K., and Otsuka, Y. (2011). Motion of polar cap arcs. *Journal of Geophysical Research: Space Physics*, 116(A1). <https://doi.org/10.1029/2010JA015906>

Milan, S. E., Hubert, B., and Grocott, A. (2005). Formation and motion of a transpolar arc in response to dayside and nightside reconnection. *Journal of Geophysical Research: Space Physics*, 110(A1). <https://doi.org/10.1029/2004JA010835>

Rairden, R. and Mende, S. (1989). Properties of 6300-Å auroral emissions at south pole. *Journal of Geophysical Research: Space Physics*, 94(A2):1402-1416. <https://doi.org/10.1029/JA094iA02p01402>

Reidy, J. A., Fear, R., Whiter, D., Lanchester, B., Kavanagh, A. J., Milan, S., Carter, J., Paxton, L., and Zhang, Y. (2018). Interhemispheric survey of polar cap aurora. *Journal of Geophysical Research: Space Physics*, 123(9):7283-7306. <https://doi.org/10.1029/2017JA025153>

Zhu, L., Schunk, R., and Sojka, J. J. (1997). Polar cap arcs: A review. *Journal of Atmospheric and Solar-Terrestrial Physics*, 59(10):1087-1126. [https://doi.org/10.1016/S1364-6826\(96\)00113-7](https://doi.org/10.1016/S1364-6826(96)00113-7)

Slide 1 image credit: Dynamics Explorer-1 / University of Iowa